MODERN ASTRONOMY:
FROM THE EARLY UNIVERSE TO EXOPLANETS AND BLACK HOLES

Study of the physical and chemical properties of dense clumps in several high-mass star-forming regions

A. Pazukhin[1,2], I. Zinchenko[1], and E. Trofimova[1]

[1] Federal Research A. V. Gaponov-Grekhov Institute of Applied Physics of the Russian Academy of Sciences, 46 Ul'yanov str., Nizhny Novgorod, 603950 Russia
[2] National Research Lobachevsky State University of Nizhny Novgorod, 23 Gagarin Ave, Nizhny Novgorod, 603950 Russia

Abstract. Massive stars play an important role in the Universe. Unlike low-mass stars, the formation of these objects located at great distances is still unclear. It is expected to be governed by some combination of self-gravity, turbulence, and magnetic fields. Our aim is to study the chemical and physical conditions of dense clumps in several high-mass star-forming regions. We performed observations towards 5 high-mass star-forming regions (L1287, S187, S231, DR 21(OH), NGC 7538) with the IRAM 30-m telescope. We covered the 2–3 and 4 mm wavelength bands and analysed the lines of HCN, HNC, HCO^+, HC_3N, HNCO, OCS, CS, SiO, SO_2, and SO. Using the astrodendro algorithm on the 850 μm dust emission data from the SCUBA Legacy catalogue, we identified dense gas clumps and assessed their masses, H_2 column densities, and sizes. Furthermore, the kinetic temperatures, molecular abundances and dynamical state were obtained. The Red Midcourse Space Experiment Source survey (RMS) was utilized to identify the types of clumps. A total of 20 clumps were identified. We found no significant correlation between line width and size, but the linewidth-mass and mass-size relationships are strongly correlated. Virial analysis indicated that the clumps with H II regions and young stellar objects (YSOs) are gravitationally bound. Furthermore, it was suggested that significant magnetic fields provide additional support for clump stability. Molecular abundances show a decreasing trend from YSOs to submm and H II regions.

Keywords: ISM: abundances, molecules; stars: formation, massive; astrochemistry

DOI: 10.26119/VAK2024.080

1 Introduction

High-mass stars (also OB stars, $L > 10^3\,L_\odot$, $M > 8\,M_\odot$) play an important role in the Universe via their feedback. Their formation and evolution are still unclear. According to the review by Zinnecker & Yorke (2007), the evolution phase can be divided into several groups of objects. Objects associated with the initial phase of high-mass star formation are referred to as IR dark clouds (IRDCs). These clouds consist of dense and cold gas, which is believed to represent the initial conditions for high-mass star formation. Hot molecular cores (HMCs) have large masses of warm and dense gas, large abundances of complex organic and maser emission. Finally, ionised radiation from the embedded stellar population influences the parent molecular cloud, leading to the formation of an ultra-compact H II region (UCHII).

2 Observational data

In September 2019, we observed five massive star-forming regions using the IRAM 30-m radio telescope in the framework of the project No. 041-19. The list of sources is given in Table 1. Observations were carried out in the on-the-fly (OTF) mode over a mapping area of $200'' \times 200''$ and covered the 2–3 and 4 mm wavelength bands. A detailed description of the observations and data reduction is available in the published paper on deuterated molecules (Pazukhin et al. 2023). The following lines of molecules were observed: HCN (1–0), HNC (1–0), HCO^+ (1–0) and their ^{13}C isotopologues, HC_3N (8–7), OCS (6–5), $C^{34}S$ (3–2), SiO (2–1), SO (2–1), SO_2 ($6_{0,6}$–$5_{1,5}$), and HNCO ($4_{0,4}$–$3_{0,3}$).

Table 1. List of sources.

Source	RA(J2000) hh:mm:ss	Dec(J2000) °:′:″	$V_{\rm lsr}$ km/s	d kpc	$R_{\rm GC}$ kpc
L1287	00:36:47.5	63:29:02.1	−17.7	0.93	8.64
S187	01:23:15.4	61:49:43.1	−14.0	1.44	9.06
S231	05:39:12.9	35:45:54.0	−16.6	1.56	9.67
DR 21(OH)	20:39:00.6	42:22:48.9	−3.8	1.50	8.04
NGC 7538	23:13:44.7	61:28:09.7	−57.6	2.65	9.48

3 Results

To extract the clumps, we use Python `astrodendro`[1] (Rosolowsky et al. 2008). A dendrogram is employed to represent a hierarchical data structure. The dendrogram consists of two types of structures: branches, which can be divided into branches and

[1] http://www.dendrograms.org

leaves, which represent the final structures. We define the leaves on the dendrogram as clumps. Approximately 20 clumps were identified. The RMS survey (Lumsden et al. 2013) was used to determine the clump types. Three clumps were found to be associated with the H II regions, 10 with YSOs, and 7 with submillimetre emission. Masers were identified from the maser database[2] (Ladeyschikov et al. 2019). Water, hydroxyl, and methanol masers are observed in clumps associated with YSO and H II regions.

Using 850 μm dust emission data from the SCUBA Legacy catalogue (Di Francesco et al. 2008), we analysed the masses, H_2 column density and size of the clumps. To estimate the clump masses, the following equation was used (Kauffmann et al. 2008):

$$M = 0.12\,M_\odot \left(e^{14.39(\lambda/\mathrm{mm})^{-1}(T_\mathrm{dust}/K)^{-1}} - 1\right) \frac{\kappa_\nu}{\mathrm{cm^2 g^{-1}}} \times \frac{F_\nu}{\mathrm{Jy}} \left(\frac{d}{100\ \mathrm{pc}}\right)^2 \left(\frac{\lambda}{\mathrm{mm}}\right)^3, \quad (1)$$

where the gas-to-dust ratio is assumed to be 100, λ is the wavelength, F_ν is the integrated flux, T_dust is the dust temperature, d is the distance to the object. Dust opacity $\kappa_\nu = 1.82$ cm^{2}g^{-1} at 850 μm (Ossenkopf & Henning 1994). The dust temperature was set at T_dust. As a result, the H_2 column density and density are derived as

$$N(\mathrm{H_2}) = \frac{M}{\mu_{\mathrm{H_2}} m_\mathrm{H} (\pi R_\mathrm{eff}^2)}\ ,\ n(\mathrm{H_2}) = \frac{M}{\mu_{\mathrm{H_2}} m_\mathrm{H} (4/3\pi R_\mathrm{eff}^3)},$$

where m_H is the hydrogen mass, a mean molecular weight $\mu_{\mathrm{H_2}} = 2.8$, and R_eff as the effective radius derived from the clump area $\sqrt{A/\pi}$.

The virial parameter, which compares the mass of the virial with the gas mass, offers a method to assess cloud stability. The virial parameter is defined as follows (Bertoldi & McKee 1992):

$$\alpha_\mathrm{vir} = \frac{5\sigma_\mathrm{tot}^2 R_\mathrm{eff}}{GM},$$

where G is the gravitational constant. The σ_tot is defined by the width of the observed line considering the thermal and non-thermal components.

Kinetic temperature maps were adopted from the integral intensity ratios of the $J = 1$–0 HCN and HNC and their ^{13}C isotopologues as reported by Pazukhin et al. (2023). The column density is estimated under the assumptions of local thermodynamic equilibrium conditions, the optically thin Rayleigh-Jeans approximation, and negligible background.

Larson (1981) defined the relations between linewidth, cloud mass, density, and cloud size. The Larson's laws are as follows:

(1) the velocity dispersion of clouds relative to their size, $\sigma \propto L^{0.38}$;

[2] https://maserdb.net

(2) the velocity dispersion as a function of the cloud mass, $\sigma \propto M^{0.2}$;
(3) the mean density varies with cloud size, with the relationship being $n \propto L^{-1.1}$.

Then, the mass-size relationships can be defined from (1) and (2), $M \propto L^{1.9}$.

In Fig. 1 we show Larson's relations. The results indicate a weak correlation between the $\sigma_{\rm obs}$ and L, with a Spearman's rank correlation coefficient of $r_s = 0.15$ (p-value = 0.533). We estimate the power-law index to be 0.35 ± 0.15. The correlation between $\sigma_{\rm obs}$ and M is strong ($r_s = 0.6$, p-value = 0.008), with a slope of 0.17 ± 0.05. The $n(\mathrm{H_2})$ and L show a strong anti-correlation with $r_s = -0.5$ (p-value = 0.023) and a slope of -0.81 ± 0.38. The mass and size present a strong correlation ($r_s = 0.8$, p-value $= 2.4 \times 10^{-5}$), with a power-law index of 2.2 ± 0.37.

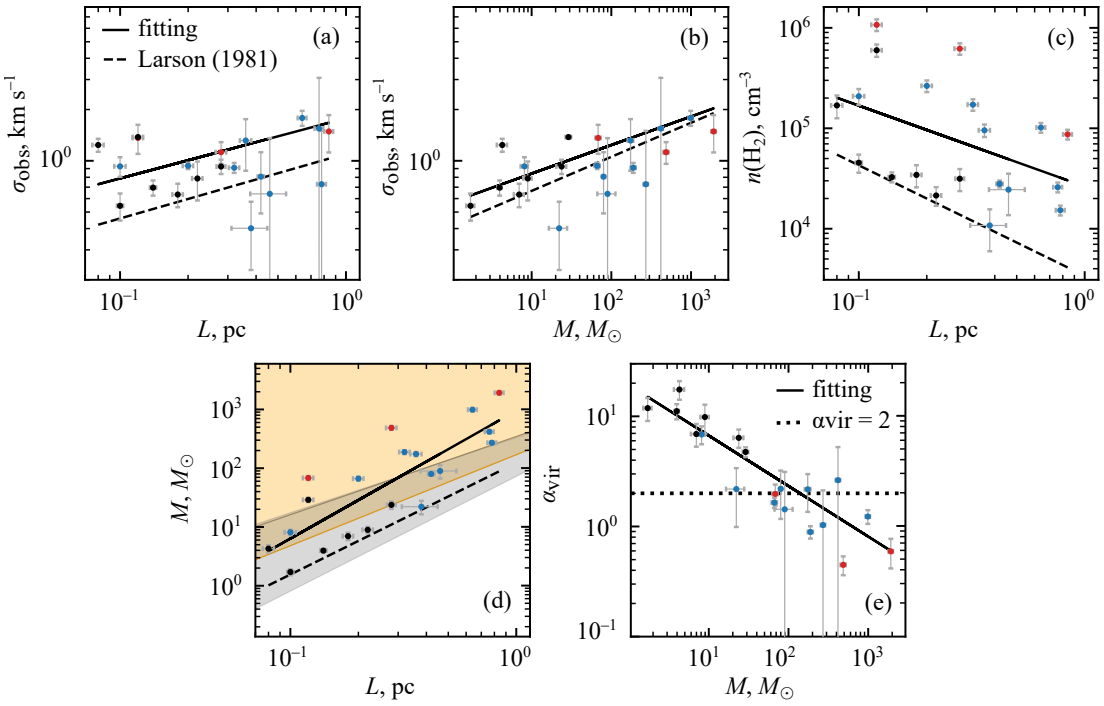

Fig. 1. The relations of $\sigma_{\rm obs}$–L (a), $\sigma_{\rm obs}$–M (b), $n(\mathrm{H_2})$–L (c), M–L (d) and $\alpha_{\rm vir}$–M (e) for clumps associated with submm emissions (black), YSOs (blue), and H II regions (red). In panel (d), the orange shading represents the area where a magnetic field is required for the stability of clumps against gravitational collapse. Region without massive star formation highlighted by gray shading (Kauffmann et al. 2013). In all panels, the black line shows the fitting result. The black dashed line illustrates the original Larson relation (Larson 1981). In panel (e), the horizontal dashed line at $\alpha_{\rm vir} = 2$ gives the critical value expected for non-magnetised clouds.

Figure 1d illustrates the relationships between mass and size, as well as the magnetic fields. The clumps containing YSO and H II regions are found within a magnetic

field region ($B > 0$ μG) and show a low virial parameter ($\alpha_{\rm vir} < 2$). The density and mass of these clouds are such that the thermal pressure and random gas motions do not provide substantial support against self-gravity. This is evidenced by a low virial parameter, which suggests that magnetic fields provide additional support.

Figure 2 illustrates averaged molecular abundances for different clump types. It was observed that molecular abundances decrease from clumps with YSOs to submm and H II regions. The maximum abundance was obtained for HCN (about 10^{-9}), and decreased to approximately 10^{-11} for SiO. Yu & Xu (2016) conducted an investigation of 87 RMS sources. The abundances of N_2H^+, C_2H, HC_3N, and HNC do not show a significant difference between MYSOs and H II regions. Gerner et al. (2014) observed a sample of 59 sources and modelled the chemical evolution. The abundances have increased with the evolutionary phase. Complex and heavy molecules decrease during the UCHII stage. In general, the molecular abundances agree with our results, assuming uncertainties of about 10.

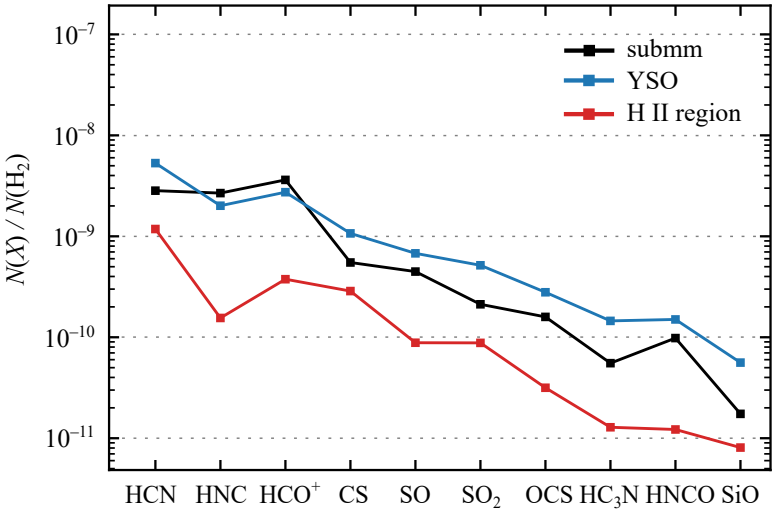

Fig. 2. The mean abundances relative to H_2 for clumps associated with submm emissions (black), YSOs (blue), and H II regions (red).

4 Summary

This work examines the physical and chemical conditions of five high-mass star-forming regions, using observations from the IRAM 30-m radio telescope. The results are as follows:

1. We identified 20 clumps. Three clumps were found to be associated with the H II regions, 10 with YSOs, and 7 with submillimetre emission. The clumps have

typical sizes of around 0.2 pc and masses in range of approximately 100 $M_\odot$ to 1000 $M_\odot$, with kinetic temperatures of about 20 K to 40 K and line widths of roughly 2 km/s.
2. We found no significant correlation between line widths and sizes, but the linewidth-mass and mass-size relationships are strongly correlated. Virial analysis indicated that the clumps with H II regions and YSOs are gravitationally bound. Virial parameter dependence on the mass of $\alpha_{\rm vir} \propto M^{-0.5}$. Furthermore, it was suggested that significant magnetic fields provide additional support for clump stability.
3. The molecular abundances decrease from clumps with YSOs to submm and H II regions. The maximum abundance was obtained for HCN (about 10^{-9}), and decreased to approximately 10^{-11} for SiO.

Acknowledgements. The research is based on observations made by the project No. 041-19 with the 30-m telescope. IRAM is supported by INSU/CNRS (France), MPG (Germany) and IGN (Spain). This paper also made use of information from the RMS survey data base at http://rms.leeds.ac.uk/ which was constructed with support from the Science and Technology Facilities Council of the UK.

Funding

This study was supported by the Russian Science Foundation project No. 24-12-00153.

References

Bertoldi F. and McKee C.F., 1992, Astrophysical Journal, 395, p. 140
Di Francesco J., Johnstone D., Kirk H., et al., 2008, Astrophysical Journal Supplement Series, 175, 1, p. 277
Gerner T., Beuther H., Semenov D., et al., 2014, Astronomy & Astrophysics, 563, id. A97
Kauffmann J., Bertoldi F., Bourke T.L., et al., 2008, Astronomy & Astrophysics, 487, 3, p. 993
Kauffmann J., Pillai T., Goldsmith P.F., 2013, Astrophysical Journal, 779, 2, p. 185
Ladeyschikov D.A., Bayandina O.S., Sobolev A.M., 2019, Astronomical Journal, 158, 6, p. 233
Larson R.B., 1981, Monthly Notices of the Royal Astronomical Society, 194, p. 809
Lumsden S.L., Hoare M.G., Urquhart J.S., et al., 2013, Astrophysical Journal Supplement, 208, 1, id. 11
Ossenkopf V. and Henning T., 1994, Astronomy & Astrophysics, 291, p. 943
Pazukhin A.G., Zinchenko I.I., Trofimova E.A., et al., 2023, Monthly Notices of the Royal Astronomical Society, 526, 3, p. 3673
Rosolowsky E.W., Pineda J.E., Kauffmann J., et al., 2008, Astrophysical Journal, 679, 2, p. 1338
Yu N. and Xu J., 2016, Astrophysical Journal, 833, 2, id. 248
Zinnecker H. and Yorke H.W., 2007, Annual Review of Astronomy & Astrophysics, 45, 1, p. 481